Small d-spacing WSi_2/Si multilayers for X-ray monochromators

Qiushi Huang (黄秋实)[1], Haochuan Li (李浩川)[1], Jingtao Zhu (朱京涛)[1*], Zhanshan Wang (王占山)[1], and Yongjian Tang (唐永建)[2]

[1]*Key Laboratory of Advanced Micro-structural Materials, Ministry of Education, Institute of Precision Optical Engineering, Physics Department, Tongji University, Shanghai 200092, China*

[2]*Research Center of Laser Fusion, Chinese Academy of Engineering Physics, Mianyang 621900, China*

Corresponding author: jtzhu@tongji.edu.cn

Received May 8, 2012; accepted July 10, 2012; posted online November 30, 2012

A WSi_2/Si multilayer, with 300 bi-layers and a 2.18-nm d-spacing, is designed for X-ray monochromator application. The multilayer is deposited using direct current magnetron sputtering technology. The reflectivity of the 1st-order Bragg peak measured at $E = 8.05$ keV is 38%, and the angular resolution ($\Delta\theta/\theta$) is less than 1.0%. Fitting results of the reflectivity curve indicate a layer thickness drift of 1.6%, mainly accounting for the broadening of the Bragg peaks. The layer morphology is further characterized by transmission electron microscopy, and a well-ordered multilayer structure with sharp interfaces is observed from the substrate to the surface. The material combination of WSi_2/Si is a promising candidate for the fabrication of a high-resolution multilayer monochromator in the hard X-ray region.

OCIS codes: 340.7480, 230.4170, 340.6720.

doi: 10.3788/COL201210.123401.

Multilayer monochromators are widely used in X-ray spectroscopy and scattering measurements to produce monochromatic incident radiation from a continuous spectrum[1,2]. Compared with crystals that possess a high spectral resolution of $\Delta E/E$ (10^{-4}–10^{-5})[3], multilayers can achieve a medium resolution of 10^{-2}–10^{-3}, but with more than one order higher flux. They can greatly reduce the application exposure time and improve the imaging contrast[4], which are suitable for experiments, such as micro-fluorescence[5], X-ray imaging[6], and crystallography[7]. Moreover, the multilayer period can be adjusted easily to work at different photon energies in the X-ray range.

Various multilayer monochromators are available for different applications. W-based multilayer systems, such as W/Si[8,9] and W/B_4C[10,11], are fabricated to produce ordinary monochromators with a spectral resolution of 1%–2%. Meanwhile, Al_2O_3/B_4C[12], SiC/C[13], and even C/C[14] can be used for higher resolution. Specific material combination, such as Pd/B_4C, is investigated to preserve beam quality in the imaging experiments[4]. This study mainly focused on ordinary multilayer monochromators using W-based systems. W/Si and W/B_4C multilayers can produce high reflectance and high flux because of their smooth growth quality even with an ultra-small layer thickness below 2 nm. However, these systems present several disadvantages. The W/B_4C multilayer has a large compressive stress[15], and the W/Si multilayer also shows an unstable stress property[16]. These conditions may cause adhesion failures during the deposition of high-resolution multilayers with a large number of bi-layers. In addition, the W/Si and W/B_4C materials have high optical contrast, limiting their theoretical spectral resolution[17]. WSi_2/Si has been utilized to fabricate multilayer mirrors because of its sharp interfaces[18] and good thermal stability[19]. It shows a more stable stress property, which is suitable for the fabrication of thick multilayer optics[6,20]. The lower optical contrast of WSi_2/Si also enables it to theoretically achieve a higher spectral resolution and show better suppression of the background radiation[21]. Thus, WSi_2/Si has emerged as a new material combination for the fabrication of multilayer monochromators[22]. This study reports our recent progress in fabricating small d-spacing WSi_2/Si multilayer with a resolution of less than 1.0%.

The multilayer was designed at $E = 8.05$ keV to characterize the optical performance in the laboratory conveniently. Reflectivity curve was first calculated and compared with the W/Si and W/B_4C multilayers, as well as an Si(111) crystal, to analyze the theoretical property of the WSi_2/Si multilayer. All reflectivity property calculations of the multilayers were performed using the IMD software[23]. The d-spacing of all multilayers was selected such that $d = 2.0$ nm with a thickness ratio (thickness of the absorption layer to the period) of $\gamma = 0.5$. The number of bi-layers was determined by the penetration depth of the X-rays for different materials. No interface or surface roughness was considered in this calculation.

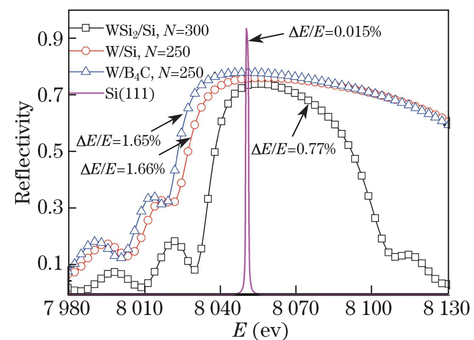

Fig. 1. Theoretical reflectivity curves of different multilayers and the Si(111) crystal. ΔE is the FWHM of each reflection peak.

 © 2012 Chinese Optics Letters

Figure 1 shows that the theoretical energy resolution of the WSi_2/Si multilayer was ~50% higher than those of the other traditional multilayers. Although Si(111) crystal exhibits the highest energy resolution of 0.015%, the integrated Bragg peak intensities of the WSi_2/Si multilayer was approximately 38 times larger than that of Si(111), indicating a much larger photon flux.

Reflectivity and angle resolution of the 1st Bragg peak for the WSi_2/Si multilayers with different d-spacing values were calculated at $E = 8.05$ keV to estimate the optimal structural parameters. The results are shown in Fig. 2. Angle resolution is defined as $\Delta\theta/\theta$, where $\Delta\theta$ is the full-width at half-maximum (FWHM) of the Bragg peak. Each multilayer consists of a saturated number of bi-layers in the calculation. The values for the interface roughness were set as 0.25 and 0.35 nm for Si-on-WSi_2 and WSi_2-on-Si, respectively, to approximate the real multilayer structure based on the reported experimental results[18]. In this study, roughness indicates the interface width of the two materials, including both the pure root-mean-square (RMS) roughness and the diffuseness. Angle resolution was significantly reduced with decreasing d-spacing because a larger number of bi-layers could be penetrated. However, a strict regularity of the large number of periodic structures is required to achieve high resolution, indicating that the deposition process must remain stable. Moreover, interface roughness has a stronger influence on reflectivity for smaller d-spacing multilayers, as shown in Fig. 2. It demands a smooth growth of the ultra-thin multilayers. Considering the optical property and difficulty of fabrication, the WSi_2/Si multilayer was first designed with $d = 2.2$ to 2.0 nm, $\gamma = 0.5$, and the number of bi-layers was $N = 300$.

The multilayer was deposited using direct current magnetron sputtering technology. The base pressure before deposition was 5.0×10^{-5} Pa. Argon gas was used as working gas during deposition, with a constant pressure of 0.2 Pa. The substrate was a super polished Si(100) wafer, with a surface RMS microroughness of ~0.3 nm (measured by an atomic force microscope).

The layer structure and optical property of the multilayer were measured after deposition via grazing incident X-ray reflectometry (GIXR) using a laboratory X-ray diffractometer. The source of the diffractometer was a sealed Cu tube followed by a Si(220) crystal monochromator to provide pure Cu Kα_1 line radiation ($E = 8.05$ keV). The divergence angle of the emitted beam was 0.007°.

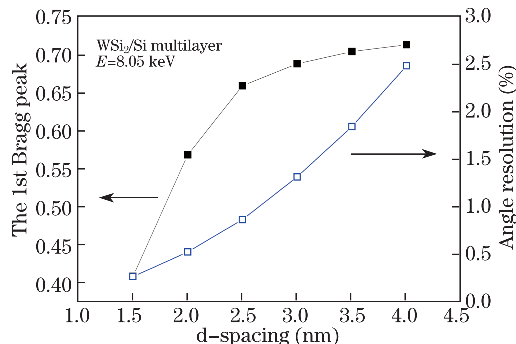

Fig. 2. Theoretical reflectivity and angle resolution of the 1st Bragg peak as a function of the multilayer d-spacing.

The deposited sample was sliced and thinned by mechanical grinding and ion milling to below 100 nm cross-section depth for high resolution transmission electron microscopy (TEM) and selected area electron diffraction (SAED) measurements to study further the layer morphology and microstructure of the WSi_2/Si multilayer. The cross-section of the multilayer was observed using a Philips EM-430 transmission electron microscope, with magnifications ranging from 880×10^3 to 420×10^3 and a point-to-point resolution of 0.23 nm.

The measured GIXR curve of the deposited WSi_2/Si multilayer is illustrated in Fig. 3. The multilayer period was calculated as $d = 2.18$ nm, based on the positions of the different Bragg peaks. The measured angle resolution of the 1st Bragg peak was 1.0%, with a reflectivity of $R = 38\%$. The discrepancy between the measured properties and the designed ones can be attributed to the interface roughness and the layer thickness drift; however, the latter is more critical for high-resolution multilayers. Layer thickness drifts are mainly caused by the instability of the deposition process, and two types of drifts are found. The systematic drift is a continuous drift through the whole multilayer stack, which mainly accounts for the broadening of the reflection peak because it gradually shifts the period from bottom to top. The other type is a random thickness error, which has less influence and affects the reflection peak shape in a chaotic manner. Both drifts will cause decreases in reflectivity as the regularity of the periodic structure is tampered[12]. Based on the principles mentioned above, the measured reflectivity curve was fitted using the IMD software to retrieve the structure parameters. The instrumental beam divergence was also considered in the fitting model because it will broaden the reflection peak in measurement.

The fitted curve is shown in Fig. 3, whereas the measured and fitted results of the 1st Bragg peak are shown separately in Fig. 4. The simulated curves fit the measured ones well, both in height and shape. The fitted results indicate a systematic thickness drift of 1.6% from the bottom to the top of the multilayer, mainly accounting for the deterioration of the angle resolution. It can be reduced by calibrating the deposition rate precisely through the whole sputtering process[24]. The random errors of layer thicknesses were within ±0.01 nm in the fitted model. Considering that the diffractometer has an instrumental beam divergence of 0.007°, it has broadened the reflectivity peak during measurement. The deposited multilayer would show a better angle resolution of below 1.0% if the incident beam was better collimated. The fitted values of the interface roughness were approximately 0.3 and 0.4 nm for Si-on-WSi_2 and WSi_2-on-Si, respectively. In this study, roughness also indicates the interface width. Layer thickness drifts together with interface roughness, causing a drop in the reflectivity for the 1st Bragg peak. The optical property and fitted structural parameters of the WSi_2/Si multilayer are listed in Table 1.

The cross-sectional TEM images of the WSi_2/Si multilayer are shown in Fig. 5. Figure 5(a) shows that high resolution image of the layer structure near the substrate, whereas Fig. 5(b) shows the layers near the surface. The dark layers are WSi_2, and the light layers are Si. Except

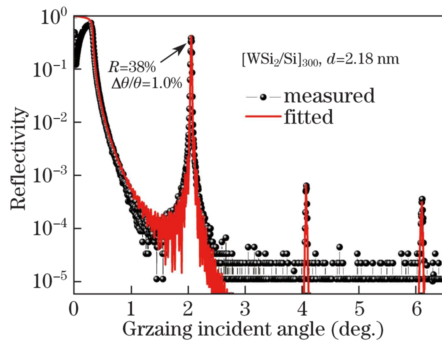

Fig. 3. GIXR curve and fitted curve of the deposited WSi_2/Si multilayer.

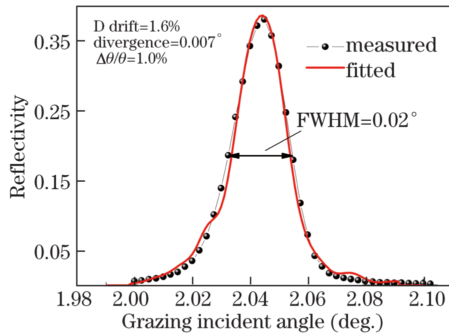

Fig. 4. Measured and fitted curves of the 1st Bragg peak of the deposited WSi_2/Si multilayer.

Table 1. Optical Property and Fitted Structural Parameters of the Deposited WSi_2/Si Multilayer

Materials	d (nm)	N	$\Delta\theta/\theta$	R_{1st}	Drift	Roughness (nm)
WSi_2/Si	2.18	300	$<$ 1.0%	38%	1.6%	0.3/0.4

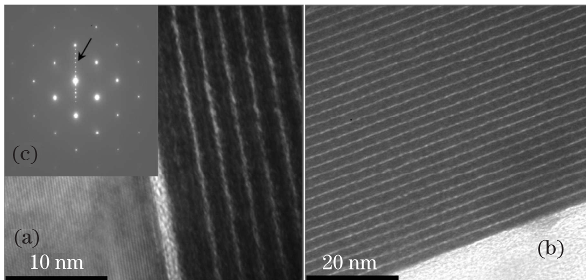

Fig. 5. TEM images of the cross-section of the WSi2/Si multilayer. Multilayer structure near the (a) substrate and (b) surface, respectively; (c) SAED pattern of the multilayer.

for the first period structure near the substrate, all layers are smoothly grown with sharp and flat interfaces that show a well-ordered multilayer structure. The small transition area between the WSi_2 and Si layers indicates a lesser inter-diffusion between the two materials, especially when compared with the W/Si system[25]. This phenomenon may account for the stable stress property of the WSi_2/Si multilayer[16]. The blurring interface of the first period can be attributed to the relatively poor quality of layers in the very initial stage of growth on the substrate. It has little influence on the performance of the entire multilayer. The individual thicknesses of the WSi_2 and Si layers cannot be determined from the TEM image because the contrast function is unknown. Figure 5(c) shows the SAED pattern of the multilayer. The strong reticular spots are the diffraction from the Si(100) substrate, and no other pattern was observed. The deposited WSi_2 and Si layers are evidently amorphous. The central string of spots indicated by an arrow corresponds to the Bragg diffraction of different orders from the periodic multilayer structure. It also indicates a good multilayer quality. According to the lattice constant of the single crystal silicon, the multilayer period was calculated as d = 2.12 nm, which was consistent with the GIXR measurement. The small difference can be attributed to the small reading errors from the SAED image.

In conclusion, the material combination of WSi_2/Si is utilized to achieve high resolution multilayer monochromators because of its stable stress property and low optical contrast. A 300-bilayer multilayer, with d-spacing of 2.18 nm, is deposited. The measured angle resolution of the 1st Bragg peak is less than 1.0% and the reflectivity is 38% at $E = 8.05$ keV. TEM measurements also show that this ultra-thin multilayer with sharp interfaces has a well-ordered structure. The fabricated WSi_2/Si multilayer can be used for high resolution multilayer monochromators in the X-ray region. However, more studies still need to be conducted to calibrate the rate drift during deposition and research the smooth growing mechanisms of the ultra-thin WSi_2/Si multilayers to improve further the spectral resolution and reflectivity.

The authors gratefully acknowledge Professor Xiaojing Wu and Dr. Xin Zhang for their help on performing the TEM measurement in the National Microanalysis Center of Fudan University. This work was supported by the National Natural Science Foundation of China (Nos. 10825521 and 10905042) and the National "973" Program of China (No. 2011CB922203).

References

1. G. Falkenberg, O. Clauss, A. Swiderski, and Th. Tschentscher, X-Ray Spectrom. **30,** 170 (2001).
2. A. Hexemer, W. Bras, J. Glossinger, E. Schaible, E. Gann, R. Kirian, A. MacDowell, M. Church, B. Rude, and H. Padmore, J. Phys. Conf. Ser. **247,** 012007 (2010).
3. P. Siddons, *Crystal Monochromators and Bent Crystals*, Handbook of Optics V, 3rd ed. (Mc Graw Hill, New York, 2010).
4. A. Rack, T. Weitkamp, M. Riotte, D. Grigoriev, T. Rack, L. Helfen, T. Baumbach, R. Dietsch, T. Holz, M. Krämer, F. Siewert, M. Meduňa, P. Cloetens, and E. Ziegler, J. Synchrotron Rad. **17,** 496 (2010).
5. R. Simon, G. Buth, and M. Hagelstein, Nucl. Instrum. Meth. Phys. Res. B **199,** 554 (2003).
6. A G. MacPhee, M W. Tate, C. F. Powell, Y. Yue, M. J. Renzi, A. Ercan, S. Narayanan, E. Fontes, J. Walther, J. Schaller, S. M. Gruner, and J. Wang, Science **295,** 1261 (2002).
7. U. Englich, A. Kazimirov, Q. Shen, D. H. Bilderback, S. M. Gruner, and Q. Hao, J. Synchrotron Rad. **12,** 345 (2005).
8. A. Rack, T. Weitkamp, S. B. Trabelsi, P. Modregger, A. Cecilia, T. dos S. Rolo, T. Rack, D. Haas, R. Simon, and T. Baumbach, Nucl. Instrum. Meth. Phys. Res. B **267,** 1978 (2009).

9. M. Stampanoni, A. Groso, A. Isenegger, G. Mikuljan, Q. Chen, D. Meister, M. Lange, R. Betemps, S. Henein, and R. Abela, in *Proceedings of Ninth International Conference on Synchrotron Radiation Instrumentation* **879,** 848 (2007).
10. R. Simon, G. Buth, and M. Hagelstein, Nucl. Instrum. Meth. Phys. Res. B **199,** 554 (2003).
11. Y. Wang, S. Narayanan, J. Liu, D. Shu, A. Mashayekhi, J. Qian, and J. Wang, J. Synchrotron Rad. **14,** 138 (2007).
12. C. Morawe, J. C. Peffen, E. Ziegler, and A. K. Freund, Proc. SPIE **4145,** 61 (2001).
13. Y. Platonov, V. Martynov, A. Kazimirov, and B. Lai, Proc. SPIE **5537,** 163 (2004).
14. A. Baranov, R. Dietsch, T. Holz, M. Menzel, D. Weißbach, R. Scholz, V. Melov, and J. Schreiber, Proc. SPIE **4782,** 160 (2002).
15. D. L. Windt, Proc. SPIE **6688,** 66880R (2007).
16. C. Liu, R. Conley, and A. T. Macrander, Proc. SPIE **6317,** 63170J (2006).
17. J. H. Underwood and T. W. Barbee, Appl. Opt. **20,** 3027 (1981).
18. Y.-P. Wang, H. Zhou, L. Zhou, R. L. Headrick, A. T. Macrander, and A. S. Özcan, J. Appl. Phys. **101,** 023503 (2007).
19. A. I. Fedorenko, V. V. Kondratenko, L. S. Palatnik, S. A. Yulin, and E. N. Zubarev, Proc. SPIE **2453,** 11 (1995).
20. Q. Huang, J. Zhu, H. Li, Z. Shen, X. Wang, Z. Wang, and Y. Tang, Chin. Opt. Lett. **10,** 013103 (2012).
21. P. Ricardo, J. Wiesmann, C. Nowak, C. Michaelsen, and R. Bormann, Appl. Opt. **40,** 2747(2001).
22. C. Liu, R. Conley, A. T. Macrander, T. Graber, Ch. Morawe, C. Borel, and E. M. Dufresne, Proc. SPIE **5537,** 154 (2004).
23. D. L. Windt, Comput. Phys. **12,** 360 (1998).
24. C. Liu, R. Conley, A. T. Macrander, J. Maser, H. C. Kang, and G. B. Stephenson, Thin Solid Films **515,** 654 (2006).
25. D. L. Windt, F. E. Christensen, W. W. Craig, C. Hailey, F. A. Harrison, M. Jimenez-Garate, R. Kalyanaraman, and P. H. Mao, J. Appl. Phys. **88,** 460 (2000).